



HAL
open science

Characterization of open woodwind toneholes by the tube reversed method

Hector Garcia Mayen, Jean Kergomard, Christophe Vergez, Philippe Guillemain, Michael Jousserand, Marc Pachebat, P. Sanchez

► **To cite this version:**

Hector Garcia Mayen, Jean Kergomard, Christophe Vergez, Philippe Guillemain, Michael Jousserand, et al.. Characterization of open woodwind toneholes by the tube reversed method. *Journal of the Acoustical Society of America*, 2021, 150 (5), pp.3763-3772. 10.48465/fa.2020.0141 . hal-03234050v2

HAL Id: hal-03234050

<https://hal.science/hal-03234050v2>

Submitted on 7 Feb 2022

HAL is a multi-disciplinary open access archive for the deposit and dissemination of scientific research documents, whether they are published or not. The documents may come from teaching and research institutions in France or abroad, or from public or private research centers.

L'archive ouverte pluridisciplinaire **HAL**, est destinée au dépôt et à la diffusion de documents scientifiques de niveau recherche, publiés ou non, émanant des établissements d'enseignement et de recherche français ou étrangers, des laboratoires publics ou privés.

Characterization of open woodwind toneholes by the tube reversed method

H. Garcia Mayén,¹ J. Kergomard,^{2, a} C. Vergez,² P. Guillemain,² M. Jousserand,³ M. Pachebat,² and P. Sanchez²

¹*Buffet Crampon, 5 rue Maurice Berteaux, Mantes-la-Ville, 78711, France*

²*Aix Marseille Univ., CNRS, Centrale Marseille, LMA UMR 7031, Marseille, France*

³*Buffet Crampon, 5 rue Maurice Berteaux1, Mantes-la-Ville, 78711, France*

(Dated: 13 October 2021)

Woodwind tonehole's linear behavior is characterized by two complex quantities: the series and shunt acoustic impedances. A method to determine experimentally these two quantities is presented for the case of open toneholes. It is based on two input impedance measurements. The method can be applied to clarinet-like instruments, and can be used for undercut toneholes as well as toneholes with pads above their output, under the condition that a symmetry axis exists. The robustness of the method proposed is explored numerically through the simulation of the experiment when considering geometrical and measurement uncertainties. Experimental results confirm the relevance of the method proposed to estimate the shunt impedance. Even the effect of small changes in the hole's geometry, such as those induced by undercutting, are characterized experimentally. The main effect of undercutting is shown to be a decrease of the tonehole's acoustic mass, in agreement with theoretical considerations based on the shape of the tonehole. Investigation on the effects of pads will be studied in a further work. Experimental results also reveal that losses in toneholes are significantly higher than those predicted by the theory. Therefore the method is suitable for the experimental determination of the shunt impedance, but it is not convenient for the characterization of the series impedance.

©2021 Acoustical Society of America. [<https://doi.org/DOI number>]

[XYZ]

Pages: 1–10

I. INTRODUCTION

For woodwind instruments, the effect of toneholes on the intonation and the ease of playing is essential. The present paper focuses on linear behaviour of open toneholes, which is especially important for the playing frequencies.

The characterization of holes can be independent of the geometry of the resonator (either cylindrical or conical, see e.g.¹).

The first theory was given by Keefe², and completed by^{4,7}. It is based on matching plane waves within the resonator and the tonehole. The tonehole is characterized by a transfer matrix of order 2. Because of reciprocity, only three elements of the matrix are necessary. Furthermore, in the present paper, the tonehole is assumed to be symmetrical, and two elements (i.e., two complex impedances) are sufficient (see⁴) for symmetrical toneholes. This can approximately happen for undercut toneholes. For toneholes with pads above their output, the radiation of the tonehole is modified, but it can be assumed that a symmetry axis exists, and two elements are also sufficient. The theory, based upon modal expansion, assumes the tonehole to be cylindrical, and this leads to a difficulty of the geometric matching between two

cylinders. However, the number and nature of the matrix elements does not depend on the shape of the toneholes, and they can be determined either by experiment or numerical discretization (see e.g.^{8–10}). The Finite Element Method can be used, but the geometric and acoustic modeling of boundary layers (see⁹) and nonlinear behaviour is not straightforward. Acoustic experiment can be also used for the computation of the input impedance of an instrument by using the transfer matrix method: the measurement of the two acoustic impedances make unnecessary the knowledge of the precise geometry. For the computation of the input impedance of an instrument, the acoustic characterization of the open toneholes is sufficient. We notice that the measured elements correspond to the pair tonehole-tube, because they depend on the tube diameter, and are useful for predicting (and maybe for optimizing) the input or transfer impedances. Moreover, the presence of pads located above the output of the open hole modifies their radiation, and therefore the shunt impedance. This paper is limited to open holes without pads, but the present method can be used for holes with pads.

Considering the equivalent circuit of an open tonehole, the elements are essentially acoustic masses. One is in series, modifying the acoustic pressure, and the other is in parallel, modifying the acoustic flow rate. They can be regarded as length corrections to the main tube and to the tonehole, respectively. Nevertheless, for high

^akergomard@lma.cnrs-mrs.fr

(i.e., long) toneholes, compressibility (and propagation) effects can appear. Moreover, for both the impedances in series and in parallel, losses (i.e., resistances) exist. Losses added to the series mass are generally ignored, and no theoretical determination exists, while experimental evidence was found by Dalmont et al¹⁰ in a nonlinear regime. At low frequencies, the two masses are almost independent of frequency, but they increase when approaching the first cutoff of the main tube. This variation has been theoretically studied only for the 2D, rectangular case (see⁴), but it is general⁵. Other shunt acoustic masses intervene, in particular that of the plane mode in the hole, and a resonance of the total shunt mass can occur at high frequency: this is detailed in Section II.

Previous articles^{6,10,14,15} used experiment devices for the measurement of the series and shunt impedances for open or/and closed toneholes, including the possibility of hole undercutting and pad existence^{6,11–14}. They took advantage of the tonehole symmetry to limit the experiment to simultaneous measurement of two quantities, the input impedance of a tube with one tonehole at its middle, and a transfer impedance. This allows avoiding dismantling the apparatus during the measurement. The present paper aims at exploring another method. It limits the measurement to two input impedances, by reversing the cylindrical tube (see Fig. 1), the extremity being open. Thus the termination impedance is unchanged when turning the tube. The drawback is the need of dismantling the set up.

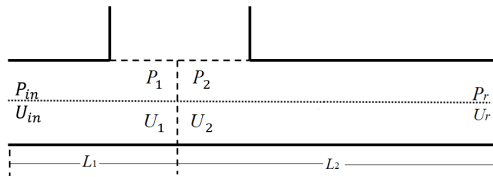


FIG. 1. Scheme of the tonehole geometry and acoustic variables. For the second situation, an apostrophe is added to the geometrical and acoustic quantities, and $L'_1 = L_2$, and $L'_2 = L_1$

In Sect. II, the calculation is performed by using the theoretical, known model of a cylindrical tonehole on a cylindrical tube. From the theoretical values of the two characteristics, the calculation determines the two input impedances of the tube in the two situations, the second being the reversed situation of the first. In Sect. III, the inverse problem (often called the crime inverse problem) is computed. It necessitates the determination of the two tonehole characteristics from the two input impedances

of the tube in two different situations. In other words two input impedances become the starting point from which the two characteristics are derived. Therefore the tube reversed method consists in reversing the tube. If the calculations are correct, the two tonehole characteristics obtained by solving the inverse problem are identical to the initial values calculated from the model.

In practice there is a very small error because of the numerical computation (direct and inverse). If some data of the inverse problem are slightly wrong, the two characteristics obtained slightly differ from the initial values. The data of the inverse problem are either geometric data or measured input impedances. Modifying these data allows assessing the sensitivity of the method to uncertainties on these data. This is the purpose of Sect. IV, which discusses some parameter choices of the experiment, such as the main tube length and the location of the tonehole.

Sect. V describes the experiment including the measurement method of the input impedance and results for cylindrical toneholes, with dimensions similar to those of a clarinet. Sect. VI presents experimental results for examples of undercut toneholes. Sect. VII discusses the validity and interest of the method.

II. DIRECT PROBLEM: MODEL OF A TUBE WITH AN OPEN TONEHOLE

The radii of the main tube and the hole are denoted a and b , respectively. The wavenumber in free space is denoted $k = \omega/c$; ω is the angular frequency, and c is the sound speed in free space. The wavenumber involving viscous-thermal losses in the main tube is given by a standard expression³ (p. 242):

$$k_a = k \left[1 + 1.044 \sqrt{-2j/r_v} - 1.08j/r_v^2 \right] \quad (1)$$

where $r_v = a\sqrt{\omega\rho/\mu}$ for the main tube. ρ is the air density, and μ the air viscosity. The same formula holds for the tonehole, with the notations k_b and b . The characteristic impedances are $Z_c = \rho c/\pi a^2$ and $Z_{ch} = \rho c/\pi b^2$. The quantities at the left (resp. right) of the tonehole are denoted with subscript 1 (resp. 2). The lengths of the main tube on the two sides of the tonehole are L_1 and L_2 . The height of the tonehole is t . The schematic of the tonehole geometry and the acoustic variables are shown in Fig. 1. In both the main tube and the tonehole, only the plane mode propagates, i.e., higher order modes are evanescent, i.e., the frequency is low enough ($k < 1.84/a$). The plane mode can be matched on the two sides of the tonehole symmetry axis by a second order transfer matrix². The effect of the tonehole is described by the following equation:

$$\begin{pmatrix} P_1 \\ U_1 \end{pmatrix} = M_h \begin{pmatrix} P_2 \\ U_2 \end{pmatrix}, \quad (2)$$

where acoustic pressure and volume velocity are denoted P and U , respectively. For the volume velocity, the axis

is oriented to the right. M_h is a symmetrical matrix with unity determinant¹⁶. It corresponds to the T-circuit (see^{3,4}) shown in Fig. 2. It is written as follows:

$$M_h = \frac{1}{1 - Y_s Z_a/4} \begin{pmatrix} 1 + Y_s Z_a/4 & Z_a \\ Y_s & 1 + Y_s Z_a/4 \end{pmatrix} \quad (3)$$

The series impedance Z_a and the shunt impedance $Z_s = 1/Y_s$ are the impedances corresponding to the anti-symmetric and symmetric parts of the velocity at the input of the tonehole^{2,3}, respectively. For an open tonehole, they are given by the following equations⁴:

$$Z_a = jkZ_c t_a \quad (4)$$

$$Z_s = jZ_{ch}(kt_i + \tan[kbt + k(t_m + t_r)]). \quad (5)$$

In the equivalent circuit and the transfer matrix the effective shunt impedance Z_h appears. It is defined by:

$$Z_h = Z_s - Z_a/4. \quad (6)$$

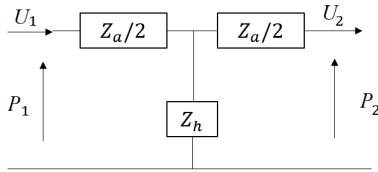


FIG. 2. Equivalent circuit for the tonehole

The lengths included in the above expressions are given hereafter. If $\delta = b/a$, the series length correction t_a is given by⁴:

$$t_a = -b\delta^2 / [1.78 \tanh(1.84t/b) + 0.94 + 0.540\delta + 0.285\delta^2]. \quad (7)$$

This quantity is very small (a typical value is 0.5 mm). For this reason several authors neglect the corresponding term in Eq. 6. However, in the matrix M_h it is not consistent to ignore a quantity in one element while keeping it in the other elements. This remark can be related to the dual role of pressure and volume velocity in Eq. (3). An important remark is that the corresponding acoustic mass is negative². No failure of causality is done, because causality is ensured by the complete matrix Eq. (3).

At low frequencies, the length t_i , due to evanescent modes, is independent of frequency and can be regarded as an internal length correction for the tonehole height. It can be written as (see⁴, and¹⁰ for a correction):

$$t_i = b(0.82 - 0.193\delta - 1.09\delta^2 + 1.27\delta^3 - 0.71\delta^4). \quad (8)$$

The length t_m is related to the matching volume between the tonehole and the main tube, and cannot be

exactly computed with the modal matching method, except when the main tube is rectangular (in which case it vanishes). Its value is given by⁷:

$$t_m = b\delta(1 + 0.207\delta^3)/8. \quad (9)$$

The length t_{rh} is the (complex) radiation length given by $t_{rh} = Z_{rh}/(jkZ_{ch})$, where rh is the subscript for the hole end, and Z_{rh} the radiation impedance of the tonehole. Different expressions exist in the literature. For the sake of simplicity, we assume that it is equal to the radiation of a tube without flange (see e.g.¹⁷). At low frequencies, the order of magnitude of the uncertainty concerning the real length correction $t_{rh} = \text{Re}(t_r)$ is $0.2b$, which is the difference between the two extreme cases (without flange and with infinite flange, respectively). If losses near the walls are ignored, the total equivalent height of the tonehole is defined as:

$$t_s = \text{Im}(Z_s/(kZ_{ch})). \quad (10)$$

At low frequencies, it is equal to:

$$t_s = t_i + t + t_m + t_r. \quad (11)$$

The geometric values chosen in this paper are the tonehole radius $b = 4$ mm (the main tube radius is $a = 7.3$ mm), and height $t = 8.5$ mm; the matching length correction is $t_m = 0.3$ mm. The length correction for radiation is $t_r = 2.5$ mm (with a significant uncertainty of $0.2b = 0.8$ mm) and the internal length correction is $t_i = 2.1$ mm. The total equivalent height is therefore $t_s = 13.4$ mm. This quantity is of major interest for the computation of the input impedance of an instrument. Using the standard transmission line theory, the effect of a tonehole height difference by 1 mm can be computed: it implies a typical shift of the first impedance peak of a typical clarinet by 0.5% to 1% (i.e., 9 to 17 cents). Therefore the cumulative shift for several toneholes can be rather high.

It remains to derive the input impedance Z_{in} . in is the subscript of the tube input, and r that of the termination. The basic equation is:

$$\begin{pmatrix} P_{in} \\ U_{in} \end{pmatrix} = M_1 M_h M_2 \begin{pmatrix} P_r \\ U_r \end{pmatrix}. \quad (12)$$

M_1 and M_2 are the transfer matrices of the cylindrical sections of the tube ($i = 1, 2$):

$$M_i = \begin{pmatrix} A_i & B_i \\ C_i & A_i \end{pmatrix} = \begin{pmatrix} \cos k_a L_i & jZ_c \sin k_a L_i \\ jZ_c^{-1} \sin k_a L_i & \cos k_a L_i \end{pmatrix}. \quad (13)$$

The terminal impedance Z_r is projected back to the right of the tonehole, as follows:

$$Z_2 = \frac{A_2 Z_r + B_2}{C_2 Z_r + A_2}. \quad (14)$$

Similarly, the impedance Z_1 at the left of the tonehole is projected from Z_2 by using the matrix M_h and Eq. (2).

Finally the input impedance Z_{in} is projected from Z_1 by using the matrix M_1 . A second choice of the lengths L_1 and L_2 lead to another value of the input impedance.

III. INVERSE PROBLEM

The aim of the inverse problem is to derive the two tonehole characteristics from the two input impedances Z_{in} and Z'_{in} . The apostrophe indicates the reverse situation. The two different situations are $L_1 < L_2$, and $L'_1 < L'_2$, when in the second case the tube is reversed such that $L'_1 = L_2$, and $L'_2 = L_1$. The tonehole is not located at the middle of the tube, in order to obtain two different input impedances when the tube is reversed. For the present method, the main tube is open: Z_r is the radiation impedance. It is assumed to be equal to its theoretical value without flange¹⁷. It was checked that the results are not very sensitive to the precise value of the radiation impedance. Using of the measured value of the radiation impedance does not change significantly the results. The important condition is that the radiation impedance is the same for the two situations. Now the input impedance is assumed to be known, and is projected back to the left of the tonehole, using the inverse matrix of M_1 as:

$$\begin{pmatrix} P_1 \\ U_1 \end{pmatrix} = \begin{pmatrix} A_1 & -B_1 \\ -C_1 & A_1 \end{pmatrix} \begin{pmatrix} P_{in} \\ U_{in} \end{pmatrix} \quad (15)$$

$$\Rightarrow Z_1 = \frac{A_1 Z_{in} - B_1}{-C_1 Z_{in} + A_1}. \quad (16)$$

Following Fig. 2, the equations for the 3 elements of the electrical equivalent circuit can be written: Defining $P = Z_h(U_1 - U_2)$; $P_1 = Z_1 U_1 = P + Z_a/2 U_1$; and $P_2 = Z_2 U_2 = P - Z_a/2 U_2$, the following equation is obtained:

$$\frac{1}{Z_h} = \frac{1}{Z_1 - Z_a/2} - \frac{1}{Z_2 + Z_a/2}. \quad (17)$$

A similar equation holds for the second situation (reversed tube), replacing Z_1 and Z_2 by Z'_1 and Z'_2 , respectively.

$$\frac{1}{Z_h} = \frac{1}{Z'_1 - Z_a/2} - \frac{1}{Z'_2 + Z_a/2}. \quad (18)$$

The following quadratic equation is obtained by eliminating Z_h :

$$AZ_a^2/4 + BZ_a/2 + C = 0, \quad (19)$$

$$\begin{aligned} A &= (Z'_1 - Z_1) - (Z'_2 - Z_2); \\ B &= 2(Z'_1 Z'_2 - Z_1 Z_2); \\ C &= Z'_2 Z_2 (Z'_1 - Z_1) - Z'_1 Z_1 (Z'_2 - Z_2) \end{aligned} \quad (20)$$

Eq. (19) can be solved for Z_a , then Z_h is derived from Eq. (17) or Eq. (18). However a simpler solution is obtained by expressing Z_h with respect to Z_a from Eq. (17). A term Z_a^2 appears. Using the latter expression and Eq. (19), and eliminating Z_a^2 , it can be written:

$$Z_a = -\frac{B}{A} - 2Z_h. \quad (21)$$

Then, introducing this result in the quadratic equation (19), the following result is obtained:

$$Z_h^2 = \frac{B^2}{4A^2} - \frac{C}{A}. \quad (22)$$

Two solutions exist for this equation. The solution with a negative real part can be eliminated because the physical system is passive. Z_s can be deduced from Eq. (6):

$$Z_s = Z_h + Z_a/4. \quad (23)$$

Throughout this paper, the results are focussed on 3 quantities: the total equivalent height of the tonehole t_s , given by Eqs. (10, 22, 23); the real part of the effective shunt impedance Z_h and the imaginary part of Z_a , from Eq. (21).

The results of the inverse problem were checked by using computed input impedances, and the order of magnitude of the numerical error is smaller than 10^{-14} . Fig. 3 shows the comparison between the direct and the inverse computations for the equivalent height of the tonehole t_s (see Eq.(10)). For Z_a , the numerical error is smaller than 10^{-12} . For other choices of termination impedance, such as an infinite impedance or the characteristic impedance, the entire computation remains valid.

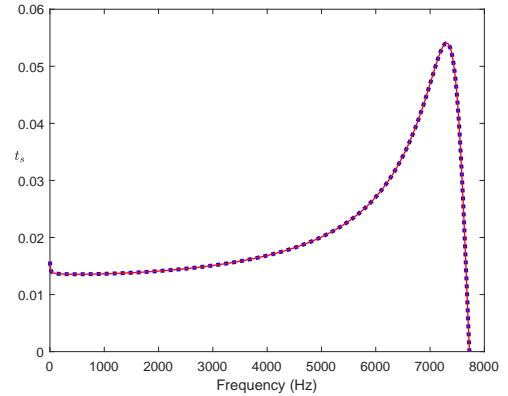


FIG. 3. (Color online) Equivalent height t_s of the tonehole (in m). Solid, red line: model; blue, dotted line: inverse problem (from Eq. (22)). Dimensions $a = 7.3$ mm, $b = 4$ mm, $t = 8.5$ mm, $L_1 = 44$ mm, $L_2 = 74$ mm.

When the frequency tends to zero, the small increase is due to the visco-thermal dispersion, which diminishes the sound speed, and increases the equivalent length. Furthermore, the strong variation at higher frequencies is due to the propagation of the planar mode in the tonehole (see the function $\tan(x)$ in Eq. (5)). The resonance near 7540 Hz corresponds to the minimum of the input impedance of the tonehole.

IV. SIMULATION OF THE EXPERIMENT

In order to simulate the experiment, errors are introduced on the data of the inverse problem. The input

impedance is first computed by using the model, and the values are treated as experimental data.

A. Effect of uncertainty on the main tube length

For the second case, an error of 0.2 mm is added to the length L_1 . It includes the uncertainty of the measurement, and the uncertainty on the tube manufacture. For the second case, an error of 0.2 mm on the length L_1 is considered together with an opposite error on the length L_2 (the later case corresponds to an error on the location of the tonehole, without change in the total length $L_1 + L_2$).

For the equivalent height of the hole t_s , Fig. 4 shows the comparison between results for the two cases simulated and the theoretical result (without errors introduced). Between 1550 Hz and 1650 Hz, the error on the result is very large. Because this also happens at other higher frequencies, the figure is limited to 2000 Hz.

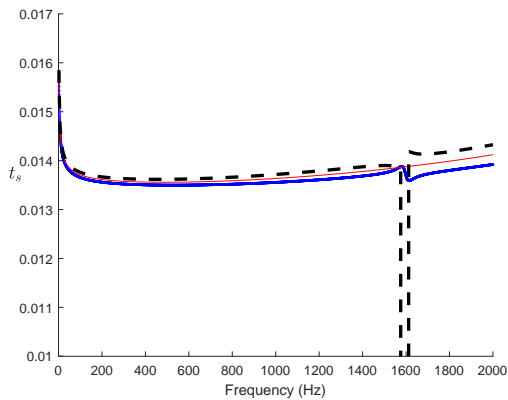


FIG. 4. (Color online) Equivalent height t_s (in m). Red, solid thin line: theory without length errors. Blue, thick, solid line: inverse problem (Eq. (22)) with 0.2 mm error on L_1 . Black, dashed line: inverse problem with 0.2 mm error on L_1 and -0.2 mm error on L_2 .

The frequency ranges with large error are close to the input impedance minima of the main tube (1560 Hz for Z_{in} and 1610 Hz for Z'_{in}). A simple qualitative interpretation is the following: suppose that the radiation impedance of the tube is 0 (whatever the frequency), and that the input impedance vanishes at a given frequency, therefore the eigenfrequencies of the tube in the two positions are equal, and the problem becomes ill-posed (one equation for two unknowns): the solutions tend to infinity. This reasoning is not exact, because the radiation impedance is small, but not 0. The variations of t_s are very small up to 1400 Hz, as well as the discrepancies with the theoretical values. Concerning the real part of the shunt impedance Z_h , it can be seen in Fig. 5 that the accuracy of the simulated results is satisfactory up to 1400 Hz.

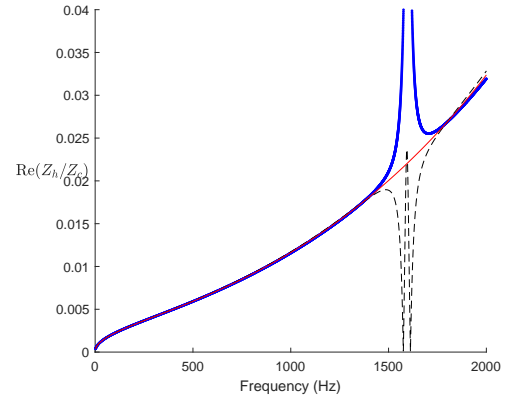


FIG. 5. (Color online) Real part of the reduced shunt impedance $Re(Z_h/Z_c)$ (dimensionless). See line definitions in the caption of Fig. 4.

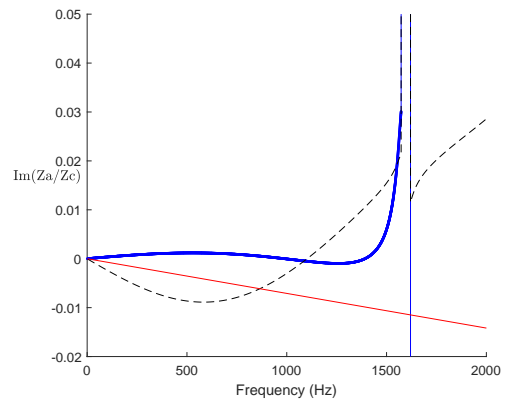


FIG. 6. (Color online) Imaginary part of the reduced series impedance $Im(Z_a/Z_c)$ (dimensionless). See line definitions in the caption of Fig. 4.

However, concerning the imaginary part of the series impedance Z_a , even a very small error on the lengths causes large errors on the result (see Fig. 6). Even the sign of the quantity is not determined. This result suggests that it is extremely difficult to expect a precise measurement of the series impedance. From this perspective, the method is less robust than the method of¹⁰, even if the later is not very precise (the uncertainty is almost 35%). The present method is probably not suitable for measuring this element through experimentation.

B. Effect of the data uncertainty on the measured input impedance

A second attempt to simulate the experiment is based on the introduction of a random error on the modulus of the input impedance (for the two configurations of the main tube Z_{in} and Z'_{in}). The input impedance is

modified as follows:

$$\widetilde{Z}_{in} = Z_{in}\{1 + 0.005[rand(N) - 0.5]\}. \quad (24)$$

The number N is the size of the input impedance vector. *rand* is a Matlab function that generates uniform pseudo-random numbers in the interval $[0, 1]$. The value 0.005 is determined by the measurement of many input impedances. It means that the error modelled ranges from -0.25% to 0.25% of Z_{in} . The three figures 7 to 9 show a confirmation of the previous observations: the measurement can be accurate up to 1600 Hz for the shunt impedance, but the measurement of the series impedance is not possible (see Figs. 7 to 9). The relative error on the equivalent height is less than 7%.

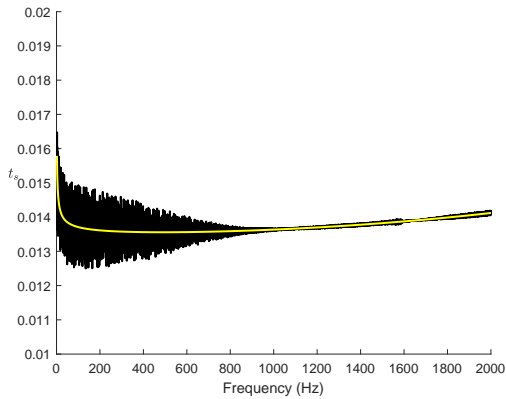


FIG. 7. (Color online) Tonehole equivalent height t_s (in m). Black lines: result of a simulation with a random error on the input impedance of the tube (Eq. 24). Yellow line: no random error.

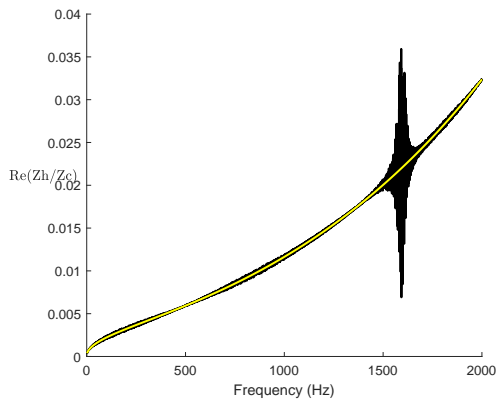


FIG. 8. (Color online) Real part of the reduced shunt impedance $Re(Z_h/Z_c)$ (dimensionless). Black lines: result of a simulation with a random error on the input impedance of the tube (Eq. 24). Yellow line: no random error.

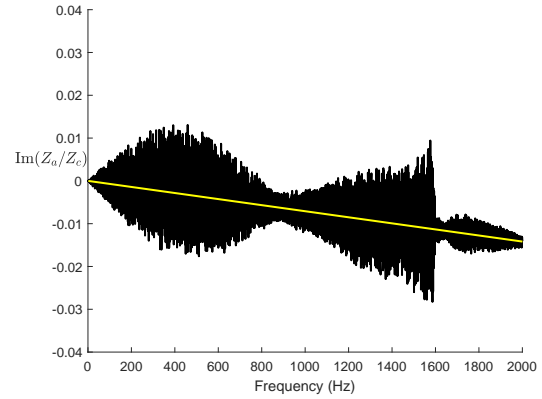


FIG. 9. (Color online) Imaginary part of the reduced series impedance $Im(Z_a/Z_c)$ (dimensionless). Black lines: result of a simulation with a random error on the input impedance of the tube (Eq. 24). Yellow line: no random error.

C. Practical considerations for the dimensions of the main tube

A conclusion of the simulation study implies that the main tube has to be chosen to be as short as possible. In order to avoid the coupling of evanescent modes between the tonehole and the radiating termination, the distance L_1 between the tonehole and the termination can be chosen between 2 and 3 times the main tube diameter. Furthermore the value of the first minimum frequency implies a small total length $L_1 + L_2$. However it is essential that the two lengths are sufficiently different, in order to avoid the quadratic equation to become degenerate. A convenient choice is L_2 between $1/3$ and $1/2$ times the total length $L_1 + L_2$. We note that other terminations for the tube lead to correct results, but, for instance, when the tube is closed, the first anti-resonance is rather low and this limits the frequency range of the measurement.

V. EXPERIMENTAL RESULTS FOR CYLINDRICAL TONEHOLES

A. Input impedance measurement

The previous analysis encourages us to study an experiment based upon the method presented in the present paper. The method is tested experimentally by using wood pieces, and the CTTM sensor¹⁸ for the impedance measurement. A piezoelectric buzzer is used as a source. The pressure in the back cavity of the buzzer is measured by a microphone, which gives an estimation of the volume velocity. The measured pipe is connected to the front of the buzzer via a small open cavity in which a second microphone measures the pressure. The input impedance of the pipe is at first order proportional to the transfer function between the two microphones. The comparison with theoretical results for cylindrical tubes

(without toneholes) is satisfactory: the discrepancy for a closed tube is 4 cents for the resonance frequencies and 1 dB for the peak heights, except at very low frequencies. For this reason, measurements are done above 200 Hz.

B. Preliminary results concerning the repeatability of the measurement

We first study the repeatability for a tube and a tonehole with dimensions equal to those previously considered. For the frequency range 200 to 1400 Hz, the equivalent height t_s of the tonehole is found to be between 14.4 mm and 15.5 mm, while the theoretical value (from Eq. 10) is 13.4 mm. For 4 measurements after disassembly and assembly, the uncertainty is found to be about 1 to 2% (see Fig. 10). Furthermore Fig. 11 shows the comparison between the measurements of 4 tubes built with the same tools. The material of the tubes is a composite material built by Buffet-Crampon for the Greenline clarinet, and the holes were deburred. The results are distributed on both sides of the theoretical one. This is an effect of the manufacturing tolerance, which is of the same order of magnitude as the measurement uncertainty, or higher. For all experimental results, the Matlab function *smooth* has been used. We remark measurements are not necessarily taken on the same day and at the same temperature, but the computation took it into account.

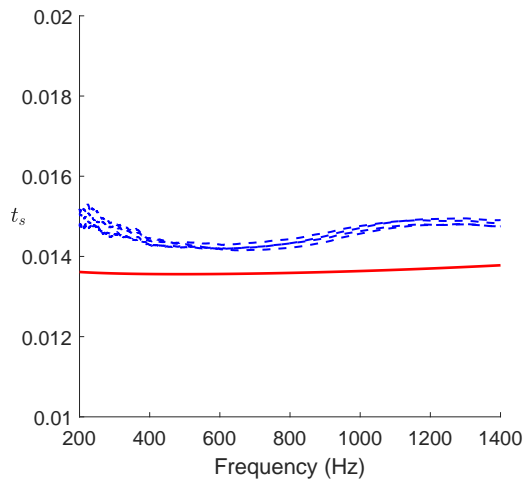


FIG. 10. (Color online) Tonehole equivalent height (in m) measured 4 times after disassembly. Blue, dashed lines: measurements. Red, solid line: theory. Dimensions $a = 7.3$ mm, $b = 4$ mm, $t = 8.5$ mm, $L_1 = 44$ mm, $L_2 = 74$ mm.

C. Comparison between two tubes of different lengths

Two tubes with the same length $L_2 = 44$ mm and with a length $L_1 = 74$ mm and 118 mm are compared. The value of L_2 is chosen to be 3 times the tube diameter.

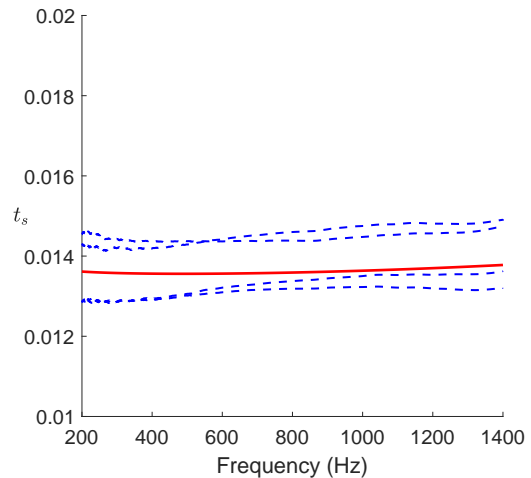


FIG. 11. (Color online) Tonehole equivalent height t_s (in m) for 4 tubes built with the same tool. Blue, dashed lines: measurements. Solid, red line: theory.

The dimensions of the tonehole are identical for the two tube lengths ($b = 4$ mm; $t = 8.5$ mm). Fig. 12 shows a small increase when the frequency approaches the eigenfrequency of the tubes. As explained above, the short tube yields better results on a wider frequency range. The discrepancy between the results of the two tubes is less than 3

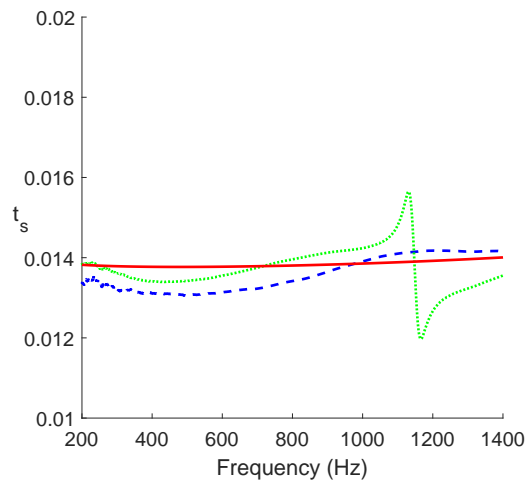


FIG. 12. (Color online) Measured value of the equivalent height t_s (in m) of the hole. Green, dashed lines: long tube. Blue, dotted line: short tube. Red, solid line: theory

Concerning the real part of the shunt impedance, it appears that the two tubes yield very similar values, except in the vicinity of the eigenfrequency. Fig. 13 shows that they are higher than the theoretical values. Remember that for a linear functioning, radiation losses are proportional to ω^2 , while visco-thermal losses increase as

$\sqrt{\omega}$. We refer to¹⁰ for a discussion about the theoretical aspects. Finally, the experiment confirms that the se-

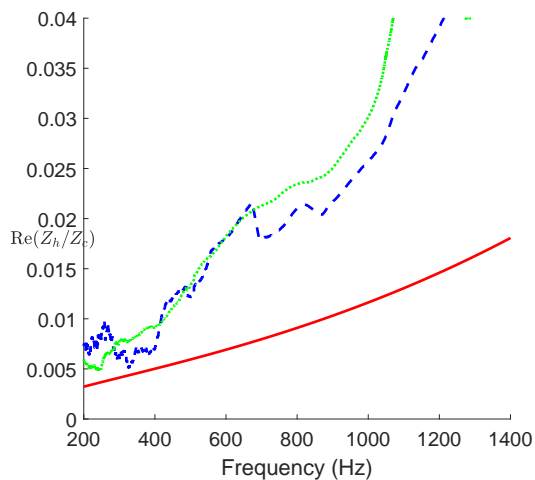


FIG. 13. (Color online) Measured value of the real part of the reduced shunt impedance $Re(Z_h/Z_c)$ (dimensionless). See the line definitions in the caption of Fig. 12.

ries impedance cannot be measured by the tube reversed method, as shown in Fig. 14.

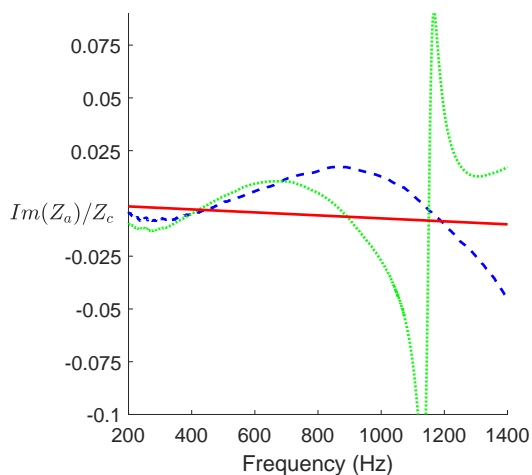


FIG. 14. (Color online) Measured value of the imaginary part of the reduced series impedance $Im(Z_a/Z_c)$ (dimensionless). See the line definitions in the caption of Fig. 12.

VI. EXPERIMENTAL RESULTS FOR UNDERCUT TONEHOLES

Undercutting toneholes was studied in¹⁰ for high excitation level and in¹⁹ (see also²⁰) for rectangular geometry. Eight short tubes of length 118 mm have holes drilled at $L_1 = 44$ mm that have three different geome-

tries: three are straight (but the hole is deburred), three are undercut with a cylinder length of 6.7 mm (tubes denoted UC1) and two are undercut with a cylinder length of 5.7 mm (tubes denoted UC2). Figs. 15 and 16 show the effect of undercutting the toneholes. The quantity shown by Fig. 15 is slightly different from that shown previously (see e.g. Fig. 13), because considering the length correction in Eq. (10) implies a division by the cross-section area S_h , but for the case of undercut toneholes, the area is not constant. For this reason, we choose the acoustic mass (per unit density) m_s :

$$m_s = Z_h/(j\omega\rho). \quad (25)$$

The figures represent the average quantities for each geometry. The effect of undercutting is a decrease of $10m^{-1}$ to $20m^{-1}$ for the acoustic mass when the undercutting becomes wider. The jump below 400 Hz in Fig. 15 remains unexplained.

Two causes for this mass increase can be analysed. The widening implies a decrease of the acoustic mass of the plane mode, and also of the internal length correction due to the discontinuity between the main tube and the tonehole. The first of these causes can be modelled. Considering the acoustic mass for the cylindrical tonehole case, calculating the average value, we obtain $280 m^{-1}$. For the cases of undercutting, we obtain $270 m^{-1}$ and $264 m^{-1}$. An elementary model can be made in order to interpret these results. The shape of the most undercut tonehole (UC2) is close to a cylinder extended in a truncated cone joining the internal wall of the main tube. For the cases studied, the lengths of the cylinder ℓ and of the cone ℓ' are approximately equal to 5.5 and 5 mm, respectively. The radius of the cylinder is $b = 4$ mm, the small radius of the cone is $R_1 = b$ and its large radius is $R_2 = 5.4$ mm. The calculation of the mass of a tube with variable cross section is done by integrating the inverse of the area along the axis. For a cone, the result is published in³, p. 325. It is that of a cylinder with a cross section equal to the geometric average of the radius: $S = \pi R_1 R_2$. The difference between the cylindrical tonehole and the undercutting one is:

$$\delta_m = \frac{\ell'}{\pi b^2} \left[1 - \frac{b}{R_2} \right]. \quad (26)$$

The result of this formula is $26m^{-1}$. This result, based on approximate geometric and acoustic models, is consistent with the experimental data. This is encouraging for the use of an accurate measurement method for the computation of the input impedance of an instrument.

Furthermore, Fig. 16 shows that the effect of undercutting on the real part of the shunt impedance is small, but significant: it causes a decrease in resistance by approximately 10 % as the undercut is increased from 0 to that of tubes UC2. It is difficult to interpret the differences between the three geometries and their variation with frequency, and the influence of nonlinear effects cannot be ignored. However, a linear reasoning can be applied here: undercutting a tonehole broadens the effective radius, and visco-thermal effects diminish.

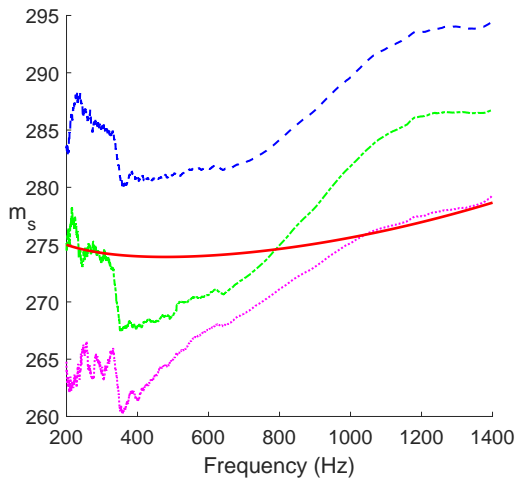


FIG. 15. (Color online) Measured value of the acoustic mass per unit density m_s of the hole. Red, solid line: theory of a cylindrical tonehole in m^{-1} . From top to bottom, 3 geometries of the tonehole: Blue, dashed line: no undercutting; Green, dash-dot line: undercut tubes UC1, Magenta, dotted line: undercut tubes UC2.

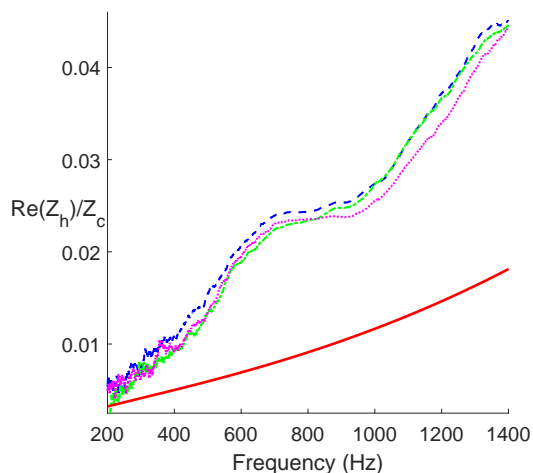


FIG. 16. (Color online) Measured value of the real part of the reduced shunt impedance $Re(Z_h/Z_c)$ (dimensionless). Red line: theory of a cylindrical tonehole. See line definitions in the caption of Fig. 15.

VII. CONCLUSION

The method presented in this paper allows an evaluation of the effect of the complex shunt impedance of an open tonehole. We recall that the aim is to insert the experimental value in the computation of the input impedance of an instrument. The effect of a hole modification on the input impedance of an instrument is significant: a difference of 1 mm for the equivalent height may imply a shift of the first impedance peak. The cumula-

tive shift for several toneholes can be rather high (see e.g. an article on the clarinet tuning¹⁶).

It is important to use a short tube for this method, due to anti-resonances associated to the total tube length. We remark that a similar problem concerning the “forbidden” frequency ranges is encountered in other methods. Moreover the distance of the hole to the tube end needs to be short.

Concerning the real part of the shunt impedance, the results appear to be robust, and suggest further studies on the theoretical aspects, even for cylindrical toneholes in the linear regime.

Concerning the equivalent height of the tonehole (related to the imaginary part of the shunt impedance), the primary quantity studied here, the results seem to be very sensitive to small geometric differences. The relative variation of the equivalent height with frequency is small, and the absolute variation remains small. For a cylindrical tonehole, at approximately 500 Hz, the discrepancy between experiment and theory is very small for the equivalent height (0.5 mm), and is of the same order of magnitude as the result obtained in¹⁰. The paper is limited to the frequency range [200 Hz, 1400 Hz] for the measurements. It is concluded that the variation with frequency is mainly due to the measurement method. Assuming that the true value of the tonehole equivalent height is independent of frequency, the choice of an average of the values between 400 and 600 Hz as appropriate can be extended to any hole geometry. This result of the different cases examined in the present work can be used for including the acoustic characteristics of undercut toneholes in a computation of input impedances of an instrument.

The method is not convenient for measuring the series impedance. Actually this quantity is very small, but for this quantity the methods proposed in previous publications seem to be better. Concerning undercut toneholes, which are generally not symmetrical, in certain cases it could be useful to search for a circuit with 3 unknowns (see⁴). The aim of the present paper is not to improve a model, but it is useful in that it highlights some of the complications inherent in existing open tonehole models. The main improvement to existing models could be done on the radiation impedance of a tonehole, including the influence of the pads.

ACKNOWLEDGEMENTS

The authors gratefully thank the French Association Nationale de la Recherche et la Technologie for the PhD grant of Hector Garcia (CONVENTION CIFRE N° 2017 1600), as well as the french Agence Nationale de la Recherche, through the joint laboratory “Liamfi” between the Laboratoire de Mécanique et d’Acoustique and Buffet Crampon (ANR LCV2-16-007-01). Furthermore the authors thank the Consejo Nacional de Ciencia y Tecnología Políticas de Privacidad Acceso (Conacyt) for the International Scholarship 707987. The authors thank Thierry Mialet (Buffet Crampon company) for designing

and manufacturing the wood pieces used in this article. Erik Petersen provided a careful reading of the English of the paper and gave useful comments, and Fabrice Silva helped for the experiment: they deserve the thanks of the authors.

¹E. Petersen, T. Colinot, J. Kergomard, P. Guillemain, “On the tonehole lattice cutoff frequency of conical resonators: applications to the saxophone”, *Acta Acust.* 4 13 (2020). DOI: <https://doi.org/10.1051/aacus/2020012>

²D.H. Keefe, “Theory on the single woodwind tone hole”, *J. Acoust. Soc. Am.* 72(3), 676–687 (1982).

³A. Chaigne, J. Kergomard, “Acoustics of musical instruments”, Springer Verlag, New York (2016).

⁴V. Dubos, J. Kergomard, A. Khettabi, J.P. Dalmont, D.H. Keefe, C. Nederveen, C. “Theory of sound propagation in a duct with a branched tube using modal decomposition”, *Acust. Acta Acust.* 85, 153–169 (1998).

⁵N. Marcuwitz, “Waveguide Handbook”, Mc Graw Hill, New York (1948).

⁶J.W. Coltman, “Acoustical analysis of the Boehm flute”, *J. Acoust.Soc. Am.*65(2), 499–506 (1979).

⁷C.J. Nederveen, J.K.M. Janssen, R.R. Van Hassel, “Corrections for woodwind tone-hole calculations”. *Acustica*, 85 957-966 (1998).

⁸P. A. Dickens, “Flute acoustics, Measurement, modelling and design”, Ph. D. Thesis, University of South Wales (2007).

⁹A. Lefebvre, G. Scavone, “Characterization of woodwind instrument toneholes with the finite element method” *J. Acoust. Soc. Am.* 131, 3153–3163 (2012).

¹⁰J.P. Dalmont, C.J. Nederveen, V. Dubos, S. Ollivier, V. Méserette, E. te Sligte, “Experimental determination of the equivalent circuit of an open side hole: linear and non linear behaviour”. *Acta Acust. United Acust.* 88, 567–575 (2002).

¹¹A.H. Benade and J.S. Murday, “Measured end-correction for woodwind tonehole”, *J. Acoust. Soc. Am.*, 41, 1609-1609 (1967).

¹²A.H. Benade, “Fundamentals of Musical Acoustics”, Oxford University Press (1976).

¹³D.H. Keefe, “Acoustic streaming, dimensional analysis, of nonlinearities, and tone hole mutual interactions in woodwinds”, *J. Acoust.Soc.Am.* 73, 1804-1820 (1983).

¹⁴D.H. Keefe, “Experiments on the single woodwind tone hole”, *The Journal of the Acoustical Society of America* 72, 688 (1982); <https://doi.org/10.1121/1.388249>

¹⁵J.P. Dalmont, “Acoustic measurement, part II: a new calibration method”, *J. Sound Vib.*, 243, 441-459 (2001).

¹⁶V. Debut, J. Kergomard, F. Laloë, “Analysis and optimisation of the tuning of the twelfths for a clarinet resonator”. *Applied Acoustics* 66, 365-409 (2005).

¹⁷F. Silva, P. Guillemain, J. Kergomard, B. Mallaroni, A.N. Norris, “Approximation formulae of the acoustic radiation impedance of a cylindrical pipe”, *J. Sound Vib.*, 322, 255-263 (2009).

¹⁸A. Macaluso, J.P. Dalmont, “Trumpet with near-perfect harmonicity: Design and acoustic results”, *J. Acoust. Soc. Am.* 129, 404 (2011); <https://doi.org/10.1121/1.3518769>

¹⁹R. MacDonald, “A Study of the Undercutting of Woodwind Toneholes Using Particle Image Velocimetry”, PhD Thesis, University of Edinburgh (2009). http://www.acoustics.ed.ac.uk/wp-content/uploads/Theses/Macdonald_Ro

²⁰M. Temiz, I. Lopez Arteaga, A. Hirschberg, “Nonlinear behavior in tone holes in musical instruments: an experimental study”, Conference CFA/Vishno, Le Mans 1-6 (2016).